High Stability Lateral Guided Method for Articulated Vehicle Based on Sensor Steering Mechanism

Yoshihiro Takita, Shinya Ohkawa and Hisashi Date

***Abstract* - This paper proposes SSM (Sensor Steering Mechanism) for a lateral guided vehicle with an articulated body. Authors demonstrated the simple lateral guiding method SSM for the front wheel steer type, the reverse phase four-wheel steer type and the rear wheel steer type vehicle. SSM presents the stable lateral guiding performance for automated vehicle which follows a straight and curved path created by guideway. The other hand, SSM is not established for articulated vehicles such as wheel loaders and dump trucks used in the mine and construction site. This paper leads SSM for an articulated vehicle with arbitrary position of articulation joint and develops an experimental robotic vehicle with proposed SSM. Simulated and experimental data show the advantages of proposed SSM.**

***Keywords* - Mobile robot, SSM, Articulated vehicle, Line following, Dynamics**

I. INTRODUCTION

AGVs (Automated Guided Vehicle) are used in various fields for the labor cost saving. The problem is the moving stability of the vehicle in the lateral direction resulting from dynamical characteristics by the sensor position and controlling mechanism. The lateral stability of lateral guided vehicles are investigated by Abe[1], Minami[2], Makino[3], Shladover [4] and Tsunashima [5]. A practical speed limit of the AGV used in manufacturing factory is far lower than the drift speed of the tire. The DMT (Dual Mode Truck) has a lateral instability because of the geometry of guiding mechanism. In 2005 through 2007, the DARPA (Defense Advanced Research Projects Agency)[6] held the grand challenge which spurred many robotics researchers to develop the autonomous vehicle.

This paper is focusing on industrial vehicles which are use in the construction field, an open mine, etc. In 2008 Komatsu Ltd. starts to operate an unmanned large-scale and steering-type dump truck system at the mine in Chile. This is an automated driving system by using the high accurate GPS, GYROs and Millimeter wave scanners. It will be necessary to automate the loading work in the near future. The lateral guiding system for the articulated vehicle such as a wheel loaders are investigated by Atafini[7], Bigras[8], Ridley[9], Marshall[10] and Ishimoto[11]. The automated loading is demonstrated by Koyachi[12]. Their group calculated the articulation angle under the condition without slipping. It is need to take into account the side slip of tires when the moving speed is increased. To improve the work efficiency for the automated wheel loader the stable and simple lateral guiding method for the articulated vehicle is needed.

Authors proposed and demonstrated SSM (Sensor Steering Mechanism) for the front wheel vehicle[13], the four-wheel steering vehicle with reverse phase mechanism[14-17] and the rear wheel steering vehicle[18]. When the vehicle is guided by SSM, no speed limit exists on the straight line travel, except with respect to the over steer characteristics[13]. Experimental results obtained using the developed robotic vehicle revealed that the SSM follows the guideway while adjusting the centrifugal force and the side force of the tires when traveling around corners. For the accurate simulation of vehicle moving at high speed, the authors proposed the variable kinetic friction model of the tire and applied it to the derived dynamical equations. The existence of the sensor arm prevents the application of SSM to the vehicle operating on ordinary road. The senser arm was replaced with a miniaturized 1kHz intelligent camera from 2005. The last paper pays attention to the lateral guide of a wheel loader of which articulation joint is located at the center, because SSM is not applied yet. For the first time application of the articulated vehicle authors are derived SSM for center articulated type vehicle and developed experimantal setup. Experimental and simulation results of high-speed moving are presented and demonstrated the performance of proposed method.

This paper extends the SSM method to the arbitrary position of articulation joint and develops a 1/25 scaled articulated dump truck controlled by SSM. Experimental and simulation results shows the stable high-speed moving and the performance of proposed method.

II. SSM AND DYNAMICAL MODEL

A. Sensor Steering Mechanism(SSM)

SSM for the articulated vehicle is divided into a rear wheel and a front wheel basis. For the rear wheel basis, the center of rear axis is moving over the guideway. The front wheel basis is the center of front axis is staying on the guideway. These relation is able to use for forward and backward moving of the vehicle. Figure 1 and 2 show schematic of SSM for articulated vehicle with the rear wheel and front wheel basis, respectively. For the convenient these figures are used bicycle model.

Yoshihiro Takita, Department of Computer Science, National Defense Academy, Japan(e-mail: takita@nda.ac.jp)
Shinya Ohkawa, Department of Computer Science, National Defense Academy, Japan (e-mail: em50045@nda.ac.jp)
Hisashi Date, Department of Computer Science, National Defense Academy, Japan (e-mail: date@nda.ac.jp)

ISBN: 978-988-19251-6-9
ISSN: 2078-0958 (Print); ISSN: 2078-0966 (Online)

A.1 The rear wheel basis SSM:

In Fig. 1, a point P and Q is placed at the center of front and rear wheels, respectively. E_a is a articulation joint of body. S_f is a sensor or guide roller which is located at a top of sensor arm L' form the center of the front axle, follows smoothly by the guideway of R in radius, and the angle of the sensor arm and the front body is assumed to be ϕ. The length of front and rear body form E_a are L_f and L_r, respectively. E_a is an intersection of the extension of front body. A relation between ε and ϕ is as follows:

$$L_f \sin\phi = L_r \sin\varepsilon \quad . \tag{1}$$

A linearized equation at the equilibrium point is obtained as follows:

$$\delta = \frac{L_f + L_r}{L_r}\ \phi \quad . \tag{2}$$

And the sensor arm length PS_f is

$$\overline{PS_f} = L' = L_f \cos\phi + L_r \cos\varepsilon \approx L_f + L_r = L. \tag{3}$$

This method is applied to a case that an articulation joint is located in the front half. In this case the articulation angle δ is assumed to be the virtual steering angle of front wheel vehicle, then the angle of sensor arm $P'S_f$ is 2δ. The stability analysis of the front steer type SSM is described in the previous paper, so this paper leaves out to explain precisely.

A.2 The rear wheel basis SSM

Figure 2 shows the rear wheel basis SSM when the front center axle is moving on the guideway. This method is used for the backward moving to of the articulated vehicle. In Fig.2, a point P and Q are a front and rear center of axle, respectively. E_a is a articulation joint of body. S_r is a top of sensor arm PS_r. Q' is a virtual rear wheel and an intersection of extended line PE_a and turning center O to Q. P' is an intersection of extended line PE_a and OS_r. A relation between a arm angle γ and articulation angle δ is

$$\delta = 2\gamma. \tag{4}$$

This result is able to use for an arbitrary position of articulation joint. In this case the sensor arm length has to be change by the turning radius. Then the linear approximation is applied this relation if the articulation angle is a range of small:

$$\overline{QS_r} = 2R\sin\frac{\delta}{2} \approx R\,\delta \quad , \tag{5}$$

$$\overline{PQ'} = R\tan\delta = \frac{L_f}{\cos\delta} + L_r \approx L_f + L_r \approx R\,\delta \quad . \tag{6}$$

Finally, the sensor length is able to use the same length as wheel base. When the articulation angle is located at Q' this system is as same as the rear steering vehicle. The stability analysis of straight line moving of the rear steering vehicle controlled by SSM is shown by the author. In this case this paper leaves out to explain the stability problem.

B. Dynamical Equation of Motion

Figure 3 shows the rigid body bicycle vehicle model moving at $\boldsymbol{V}$. It is assumed that the right and left tires have same characteristics. In figure 3, N is the Newton reference frame. Dextral sets of mutually perpendicular unit vectors $\mathbf{n}_1$ and $\mathbf{n}_2$ are fixed in N. The reference frame A is fixed on the vehicle,

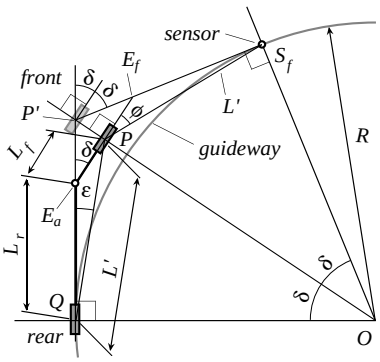

Fig. 1 Rear wheel basis SSM for articulated vehicle

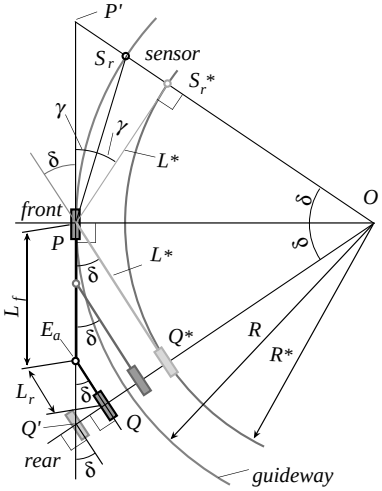

Fig. 2 Front wheel basis SSM for articulated vehicle

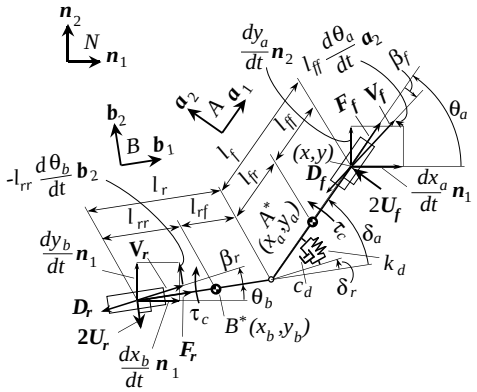

Fig. 3 Schematic model of articulated vehicle

and the mutually perpendicular unit vectors $\mathbf{a}_1$ and $\mathbf{a}_2$ are fixed in A. Here, θ is the body position angle, g is the yaw angle, δ_f and δ_r are the steering angles of the front and rear tires, respectively, β_f and β_r are the slip angles of the front and rear tires, respectively, γ_f and γ_r are the angles between $\mathbf{n}_1$ and the velocity vector of the front and rear axles, respectively. In addition, U_f and U_r are the cornering forces of the front and rear tires, respectively, l_f and l_r are the distances from the center of gravity to the front and rear axles, respectively, m is the mass, and I is the moment of inertia about the yaw-axis of the vehicle. Finally, F_f and F_r are the driving forces, and D_f and D_r are the rolling resistance forces of the front and rear tires which are acting in the opposite direction of velocity vector $\boldsymbol{V}_f$ and $\boldsymbol{V}_r$, respectively.

When the displacement vector is used as follows:

$$\mathbf{X}=[\, x \quad y \quad \theta_a \quad \theta_b \,]^{\mathrm{T}}. \tag{7}$$

The dynamical equation of motions are derived as follows:

$$\mathbf{M}\ddot{\mathbf{X}}+\mathbf{C}\dot{\mathbf{X}}+\mathbf{D}(\dot{\mathbf{X}}) = \mathbf{F} \tag{8}$$

$$\mathbf{M}=\begin{bmatrix} M_{11} & 0 & M_{13} & M_{14} \\ 0 & M_{11} & M_{23} & M_{24} \\ M_{13} & M_{23} & M_{33} & M_{34} \\ M_{14} & M_{24} & M_{34} & M_{44} \end{bmatrix}, \quad \mathbf{C}=\begin{bmatrix} C_{11} & 0 & C_{13} & C_{14} \\ 0 & C_{11} & C_{23} & C_{24} \\ C_{13} & C_{23} & C_{33} & C_{34} \\ C_{14} & C_{24} & C_{34} & C_{44} \end{bmatrix},$$

$$\mathbf{D}(\dot{\mathbf{X}}) = [D_1\, D_2\, D_3\, D_4]^{\mathrm{T}},$$

$$\mathbf{F}= [\, F_1\, F_2\, F_3\, F_4]^{\mathrm{T}}.$$

Where

$$M_{11}= -m_a-m_b \quad , \qquad M_{13}= -(l_f m_b+l_{ff} m_a) \sin\theta_a,$$

$$M_{14}= -l_{rf} m_b \sin\theta_b, \qquad M_{23}= -(l_f m_b+l_{ff} m_a) \cos\theta_a,$$

$$M_{24}= l_{rf} m_b \cos q_b, \qquad M_{33}= -I_a - l_{rf}^2 m_a - l_f^2 m_b,$$

$$M_{34}= -l_f l_{rf} m_b \cos\delta_a, \qquad M_{44}= -I_b - l_{rf}^2 m_b,$$

$$C_{11}= D_f/\sqrt{\dot{x}^2+\dot{y}^2} + D_r/E \quad , \qquad C_{13}= D_r l_f \sin\theta_a/E \quad ,$$

$$C_{14}= D_r l_r \sin\theta_b/E \quad , \qquad C_{23}= -D_r l_f \cos\theta_a/E \quad ,$$

$$C_{24}= -D_r l_r \cos\theta_b/E \quad , \qquad C_{33}= D_r l_f^2/E \quad ,$$

$$C_{34}= D_r l_f l_r \cos\delta_a/E \quad , \qquad C_{44}= D_r l_r^2/E \quad ,$$

$$D_1= (l_f m_b - l_{ff} m_a)\dot{\theta}_a^2 \cos\theta_a - l_{rf} m_b \dot{\theta}_b^2 \cos\theta_b$$

$$D_2= (l_f m_b - l_{ff} m_a)\dot{\theta}_a^2 \sin\theta_a - l_{rf} m_b \dot{\theta}_b^2 \sin\theta_b$$

$$D_3= -l_f l_{rf} m_b \dot{\theta}_b^2 \sin\delta_a, \qquad D_4= l_f l_{rf} m_b \dot{\theta}_a^2 \sin\delta_a,$$

$$F_1= 2U_f \sin\theta_a + 2U_r \sin\theta_b - F_f \cos\theta_a - F_r \cos\theta_b,$$

$$F_2= -2U_f \cos\theta_a - 2U_r \cos\theta_b - F_f \sin\theta_a - F_r \sin\theta_b,$$

$$F_3= 2U_r l_f \cos\delta_a - F_r l_f \sin\delta_b + \tau_c,$$

$$F_4= 2U_r l_r - \tau_c$$

and

$$E=\sqrt{\begin{array}{l} \dot{x}^2+\dot{y}^2+l_f^2\dot{\theta}_a^2+l_r^2\dot{\theta}_b^2+2l_f\dot{x}\dot{\theta}_a\sin\theta_a+2l_r\dot{x}\dot{\theta}_b\sin\theta_b \\ +2l_f l_r\dot{\theta}_a\dot{\theta}_b\cos\delta_a - 2l_f y\dot{\theta}_a\cos\theta_a - 2l_r y\dot{\theta}_b\cos\theta_b \end{array}}. \tag{9}$$

The control torque of PD controller is as follows:

$$\tau_c= -(\delta_a-\delta_r)k_d - \dot{\delta}_a c_d. \tag{10}$$

In this case, the cornering forces are regarded as a linear function of the slip angle and are written as follows:

$$U_f = -2K_f\beta_f \quad , U_r = -2K_r\beta_r \tag{11}$$

where K_f and K_r are the cornering power of the front and rear tires, respectively.

III SIMULATION RUNNING ON THE COURSE

A. Tire characteristics

In the previous paper, the relationship between the lateral force and the slip angle were measured using a test equipment. These data are also used in the present paper. The lateral forces generated by the tire are measured when the contact forces are set at 3.63N and 4.12N. These data are approximated to the fourth polynomial by using the least squares method as follows:

$$U_1^{static}(\beta) = -2.146\times10^{-5}\beta^4 + 1.824\times10^{-3}\beta^3 - 5.923\times10^{-2}\beta^2 + 0.958\,\beta + 8.391\times10^{-2}, \tag{12}$$

$$U_2^{static}(\beta) = -2.542\times10^{-5}\beta^4 + 2.183\times10^{-3}\beta^3 - 7.066\times10^{-2}\beta^2 + 1.118\,\beta + 5.146\times10^{-2}. \tag{13}$$

Equation (12) is equivalent to equation (13) multiplied by the contact force ratio 4.12/3.63. In this case the cornering force is proportionate to the contact force of the tires. For the simulation twice the cornering force is applied to the body because the front and rear axles have two tires.

B. Simulation conditions

The course, which consists of two semicircles of radius 0.5m connected by straight segments of 0.7m in length, was used to analyze the turning motion, including drifting, of a laterally guided vehicle by the SSM. The dynamical analysis of the vehicle was performed by integrating equations (1) to (3) with the Runge-Kutta method. While the numerical calculation of dynamical motions the contact point of the guideway and the sensor is determined, and the articulation angle is derived by using SSM relation which is proposed in this paper and applied to dynamical equations. In addition, the calculated velocity vectors and the rolling direction angle of the front and rear tires were used to determine the slip angles and cornering forces.

In order to simulate the drifting maneuver when the vehicle is turning at the corner, the variable kinetic model[15] is used in the cornering force calculation. And the other remaining simulation conditions are the same as the previous paper[19]. Simulation results of running on the test track are shown with the experimental results. Table 2 shows friction parameters which are founded in the simulation.

IV. EXPERIMENT AND SIMULATION

A. Dump truck type articulated robot vehicle

Before the designing of the articulated dump truck, the articulation position of commercially sealing dump truck are investigated. 1:3 is the most popular articulation ratio in a wheel base. Figure 4 shows an outside view of SSM robotic vehicle with articulate body which is developed for the experiment. Figure 5 shows outline and dimension of this robot. The wheel base is 0.21m, the tread is 0.135m, and the gross weight is 1.78kg. Three reflective markers are pasted at the front, rear axle and articulation joint, and are measured the positions by 3D measurement system. 1kHz CMOS camera located at the front axle follows a 0.02m white line pasted on a black face course. The physical parameters of this vehicle are shown in table 1, and are the same as in simulations.

The rotational angle of CMOS camera and articulation angle are controlled by servo motors through the deceleration gears. Rotational angle of the camera ϕ is sensed by the rotary encoder, and the target value of PD controller for articulation angle is set at $-4/3\phi$ when the rear wheel basis SSM and -2ϕ when the front wheel basis SSM. The vehicle body is a double-layered structure by flat aluminum plates and is not combined with suspension mechanism. The vehicle is equipped with tread-patterned tender rubber tires, the insides of which were filled with sponge in

ISBN: 978-988-19251-6-9
ISSN: 2078-0958 (Print); ISSN: 2078-0966 (Online)

order to produce soft contact with the load surface. The outside diameter and width of the tires were 0.059m and 0.023m, respectively. The data of the tire characteristics were measured and applied to the simulation. The power source is used Ni-MH AAA type 10 cells (12 Volt) and installed inside of the body.

B. Simulation and experimental results

Figure 6 and 7 show experiment and simulation data running on the test track when the vehicle is controlled by the rear wheel basis SSM moving at 2.5m/s. In each figure, (a) is the trajectories of front, middle and rear point, (b) is the velocity, (c) is the articulation angle, and (d) is the slip angle. And also Fig. 8 and 9 show data when the vehicle controlled by the front wheel basis SSM.

These figures show that the proposed SSMs for articulated vehicle are achieved the lateral guide at high-speed moving. In Fig. 6(a) and 7(a) the front and rear axle is passing away from the guideway. The other hand Fig. 8(a) and 9(a) show that the front tires are passing near the guideway and the drift of rear tires is reduced. The big difference between the rear and front wheel basis SSM is the minimum speed at the corner. The minimum speed is over the 2m/s in Fig. 8(b) and 9(b), and is lower the 2m/s in Fig. 6(b) and 7(b). Each slip angle data shows differences between SSMs. The slip angle of front wheel basis SSM is smaller than the rear wheel basis SSM. A slow-speed moving is not shown here, but the trajectory of rear tires by the front wheel basis SSM pass inside of the track. As a results simulated and experimental results are well coincide with each other. In these stimulations the control delay of PD-controller for the articulation angle is set at 15ms of which value is measured by the experiment.

V. CONCLUSIONS

This paper proposed SSMs which are a lateral guided method for a vehicle with articulated body. The idea of SSM are that the sensor is located at the tip of the sensor arm of which length is the same as the wheel base of vehicle, and an articulation angle is decided by SSMs relation. In this paper a SSM robotic vehicle is developed and the dynamical model of articulated vehicle is derived and calculated. The experimental and simulation results are shown that SSMs achieve the steady state tracking even if the drift condition is occurred at the corner. These results are well correspond with each other. Finally, advantages of SSM are that the system is a simple and the stable behavior is obtained. And SSMs are available for not only the front steering vehicle, reverse phase four-wheel steering and rear steering vehicle but also the articulated vehicle.

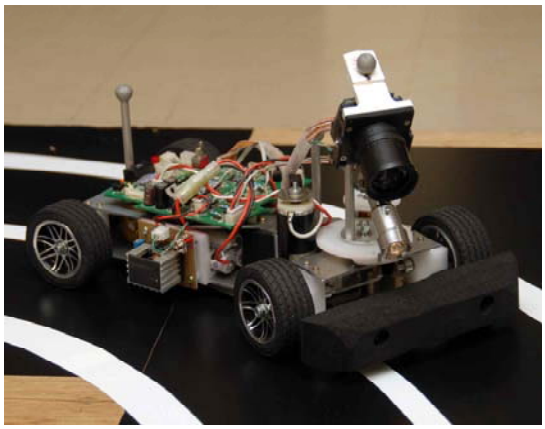

Fig. 4 Outside view of developed SSM robot vehicle

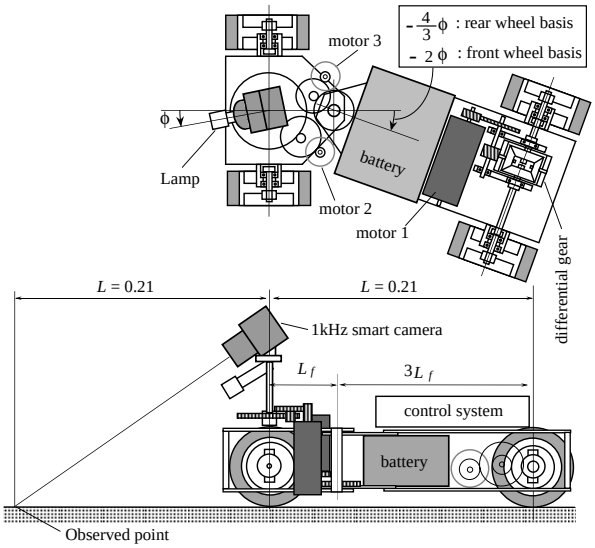

Fig. 5 Outline of constructed rear wheel steer vehicle

Table 1 Parameter of robotic vehicle

m_a	0.777	kg	m_b	0.999	kg
I_a	0.0007	kgm^2	I_b	0.0041	kgm^2
l_f	0.0525	m	l_r	0.1575	m
l_{ff}	0.02625	m	l_{rr}	0.07875	m
L	0.210	m	m	1.776	kg
W_f	9.97	N	W_r	7.38	N
k_d	40.0	Nm/rad	c_d	0.8	Nm s/rad
K_f	1.269	N/deg	K_r	1.012	N/deg

Table 2 Estimated friction parameter

	case 1	case 2	
		drift	slip
μ_f	1	0.0135	0.414
μ_k	0	0.009	0.46
T_d	-	0.0025 sec	-

References

[1] Abe, M., Vehicle Dynamics and Control, pp.192-213. kyoritsu Publication(in Japanese), 1979.

[2] Minami, M., et al., Magnetic Autonomous Guidance by Intelligent Compensation System, Vol.31, No.5, pp.382-391, 1987.

[3] Makino, T., et al., High-Speed Driving Control of an Automatic Guided Vehicle Using an Image Sensor, *Transactions of the Society of Instrument and Control Engineers*, Vol.28, No.5, pp.595-603, 1992.

[4] Shladover, S.E., et al., Steering Controller Design For Automated Guideway Transit Vehicles, *Transactions of the American Society of Mechanical Engineers*, Vol. 100, pp.1-8, 1978.

[5] Tsunashima, H., A Simulation Study on Performance of Lateral

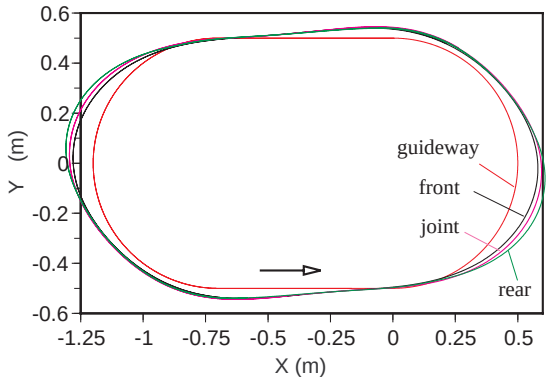

(a) loci

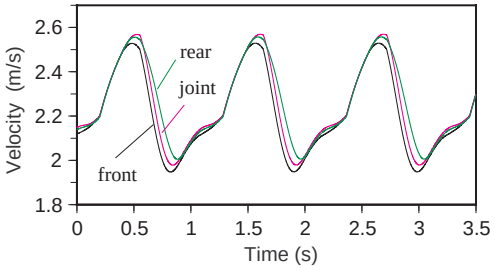

(b) velocity

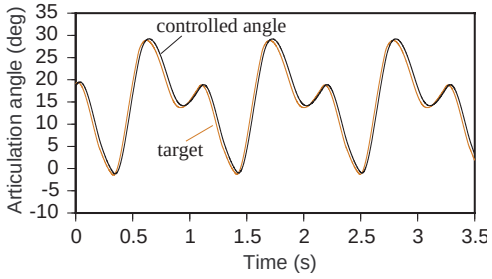

(c) articulation angle

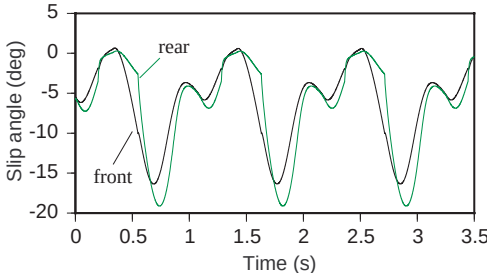

(d) slip angle

Fig. 6 Simulated data by rear wheel basis SSM at high-speed

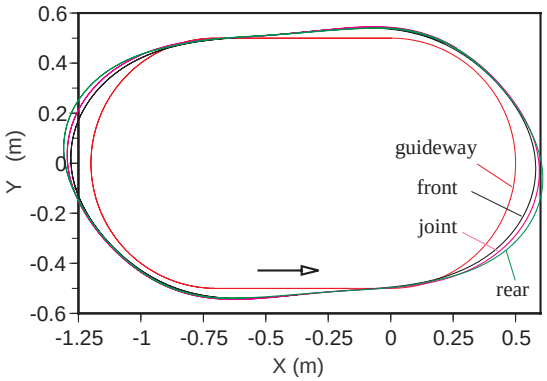

(a) loci

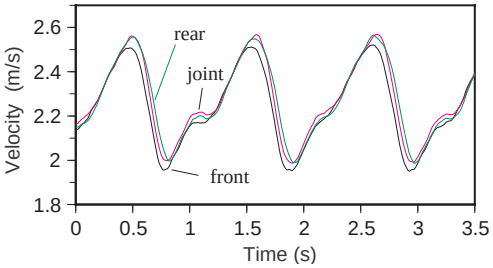

(b) velocity

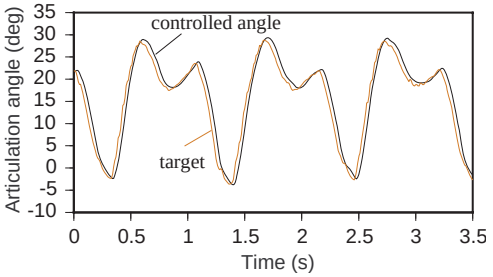

(c) articulation angle

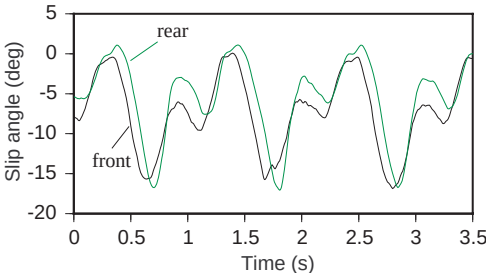

(d) slip angle

Fig. 7 Experimental data by rear wheel basis SSM at high-speed

Guidance System for Dual Mode Truck, *Transactions of the Japan Society of Mechanical Engineers* C, Vol.65, No.634, pp.2279-2286, 1999.

[6] Anhalt, C., Bagnell, J., et al., Autonomous Driving in Urban Environments: Boss and Urban Challenge, Journal of Field Robotics, Vol. 25, No. 8 (2008), pp. 425-466.

[7] Atafini, C., A Path-Tracking Criterion for an LHD Artlicuated Vchicle, *The International Journal of Robotic Research*, Vol. 18, No. 5, pp 435-441, 1999.

[8] Bigras, P., Petrov, P. and Wong, T., A LMI Approach to Feedback Path Control for an Articulated Mining Vehicle, 7th International Conference on Modeling and Simulation of Electric Machines, *Converters and Systems (Electrimacs)*, CD-ROM, 2002.

[9] Ridley, P. and Corke, P., Autonomous Control of an Underground mining Vehicle, *Proceedings of the 2001 Australian Conference on Robotics and Automation*, pp. 26-31, 2001.

[10]Marshall, J., Barfoot, T. and Larsson, J., Autonomous Underground Tramming for Center-Articulated Vehicles, *Journal of Field Robotics*, Vol. 25, No. 6-7, pp. 400-421, 2008.

[11]Ishimoto, H., Tsubouchi, T., Sarata, S. and Yuta, S., A Practical Trajectory Following of an Articulated Steering Type Vehicle, *International Conference on Field and Service Robotics*, pp.412-419, 1997.

[12]Koyachi, N. Sarata, S. and Sugawara, K., Scoop and Loading Execution by the Autonomous Wheel Loader "Yamazumi-4" -Task Control and Path Following Control -, *Journal of the Robotics Society of Japan*, Vol. 26, No. 6, pp.514-521, 2008.

[13]Takita, Y., High-speed Driving of a Lateral Guided Vehicle with Sensor

ISBN: 978-988-19251-6-9
ISSN: 2078-0958 (Print); ISSN: 2078-0966 (Online)

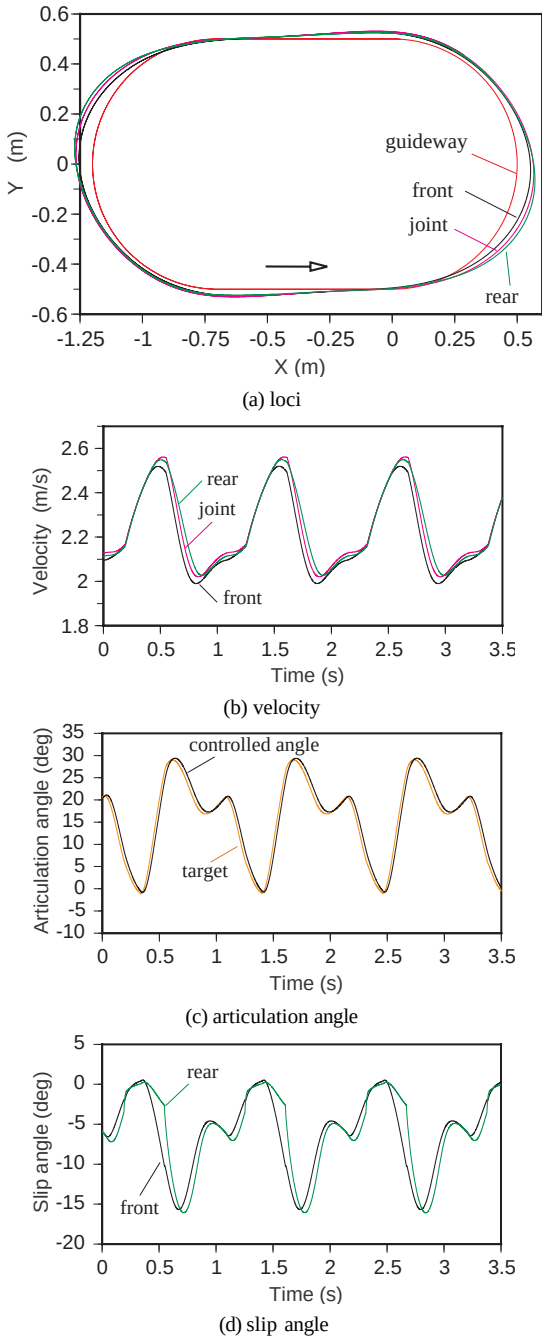

Fig. 8 Simulated data by front wheel basis SSM at high-speed

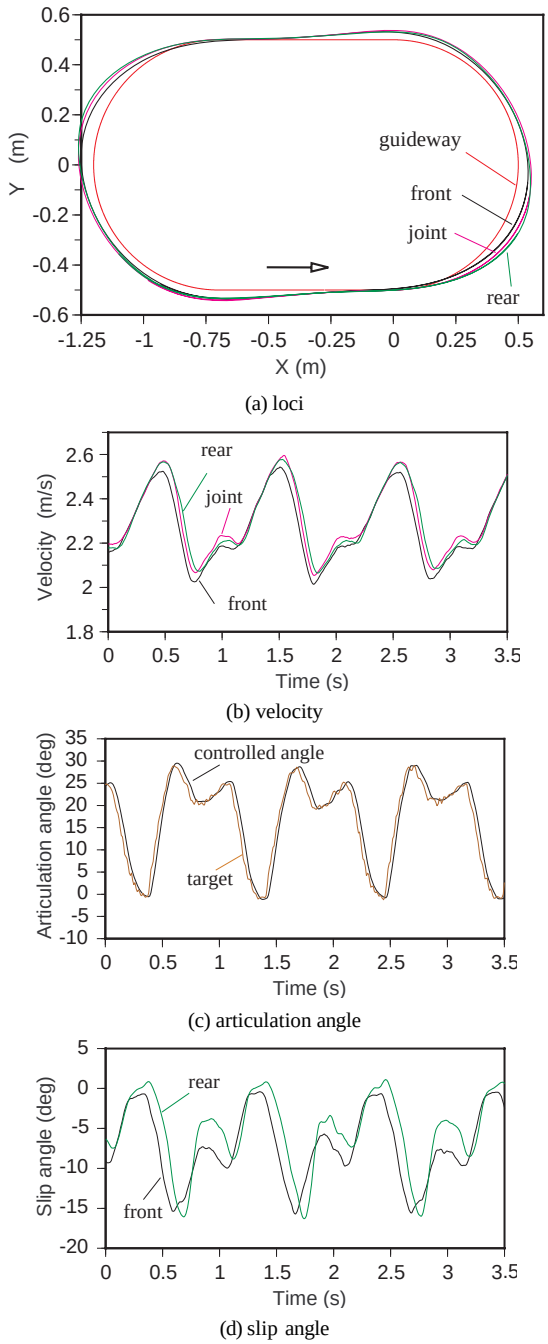

Fig. 9 Experimental data by front wheel basis SSM at high-speed

Steering Mechanism, *Transactions of the Japan Society of Mechanical Engineers C*, Vol.65, No.630, pp.622-629, 1999.

[14] Takita, Y., et al., High-speed Cornering of Lateral Guided Vehicle with Sensor Steering Mechanism, *Transactions of the Japan Society of Mechanical Engineers C*, Vol.66, No.652, pp.3888-3896, 2000.

[15] Takita, Y., Drift Turning of Lateral Guided Vehicle with Sensor Steering Mechanism(Application of a Variable Kinetic Friction Model), *Transactions of the Japan Society of Mechanical Engineers C*, Vol.68, No.675, pp.3170-3177, 2002.

[16] Takita, Y., Mukouzaka, N. and Date, H., Control of Lateral Guided Vehicle with Sensor Steering Mechanism Using Miniaturized 1kHz Smart Camera(Stabilization by Dynamic Damper), *Transactions of the Japan Society of Mechanical Engineers C*, Vol.71, No.701, pp.193-199, 2005.

[17] Takita, Y., Sakai, Y., Takahashi, T., Date, H. and Mukouzaka, N., Increasing the Speed of a Lateral Guided Vehicle with a Sensor Steering Mechanism Using 1kHz Intelligent Camera (Drift Control by Changing of Steering and Arm Length Ratio), *Transactions of the Japan Society of Mechanical Engineers C*, Vol.72, No.717, pp.1558-1565, 2006.

[18] Takita, Y. and Date, H., Dynamical Characteristics of Lateral Guided Robotic Vehicle with a Rear Wheel Steer Mechanism Controlled by Sensor Steering Mechanism, *Transactions of the Japan Society of Mechanical Engineers*, Series *C*, Vol.75, No.753, pp.1346-1353, 2009

[19] Takita, Y., Kasai, K. and Date, H., Proposition of SSM for Lateral Guided Vehicle with Articlated Body, *Transactions of the Japan Society of Mechanical Engineers C*, Vol. 76, No. 765, pp. 1130-1138, 2010.

ISBN: 978-988-19251-6-9
ISSN: 2078-0958 (Print); ISSN: 2078-0966 (Online)